ERJ
Engineering Research Journal
Faculty of Engineering
Menoufiya University

STUDY ON VERTICAL AIR CURTAINS FOR MULTI-DECK VIEWER REFRIGERATED DISPLAY

Mostafa A. Abdel-Baky* Shedeed H. Shams El-Dein* Tareq E. Shalma**

** Dept. of Mech. Power Engineering, Faculty of Engineering*
Menoufiya University, Shebin El-kom, Egypt
***Production Manager, Fricool Refrigeration Industry Company*

ABSTRACT

Air curtains are devices used in refrigerated display cabinets and the entrance of air conditioned spaces is aimed to reduce the breakthrough of heat, moisture and contaminants between the conditioned environment and the surrounding ambient, consequently reducing energy costs. The main objective of the present work is to study the parameter affecting the performance of air curtains used in viewer refrigerators using one and two air curtains at different ambient conditions, in order to reduce the air infiltration and consequently the energy consumption. The results of one and two air curtains are compared, where two air curtains are more effective than one air curtain

ملخص البحث:

تستخدم ستائر الهواء في ثلاجات العرض ومدخل الأماكن المكيفة. وتقوم ستائر الهواء بمنع انتقال الحرارة والرطوبة والأتربة بين الأماكن المكيفة أو ثلاجات العرض والجو المحيط و بناءً على ذلك تقل الطاقة المستهلكة وبالتالي تقل التكلفة.
وهدف هذه الدراسة هو دراسة العوامل المحيطة والمؤثرة على ستائر الهواء التي تستخدم في ثلاجات العرض والتى بدورها تمنع تسرب الهواء الى داخل الثلاجات وبذلك تقل الطاقة المستهلكة. وتم المقارنة بين نتائج ستارة هواء واحدة ونتائج ستارتي هواء. ومن المقارنة نستنتج أن الثلاجات التي تستخدم ستارتين يكون أداؤها أفضل.

Keywords: Air curtain, Vertical refrigerated multi-deck, Plane free jet, Heat transfer through air curtains.

1. Introduction

Display cabinets are designed to preserve the storage temperature of food. They are not able of reducing the temperature of products if they are too warm when loaded. Air curtains are devices used in refrigerated display cabinets, and the entrance of air conditioned spaces to reduce the breakthrough of heat, moisture and contaminants between the display cabinets and the surrounding ambient, which led to reduce energy costs. Forced air circulation inside display cabinets is preferable, because it is more effective in temperature distribution inside display cabinets, thus enabling the correct operation of the display cabinet. Display cabinets may use one air curtain, two air curtains or three air curtains.

In the majority of multi-deck retail display cabinets, the evaporator is located in the base of the cabinet and a fan withdraws air through it to be cooled then it passes in a duct at the rear of the cabinet. Air exits from the duct through holes or slots in the cabinet rear grille and also through a slot or a honeycomb grille placed at the front of the cabinet canopy, termed the discharge grille.
The performance of general-purpose air curtains depends on a number of parameters which include [1]:

1- The width and length of the air jet;
2- The initial jet velocity;
3- The jet initial turbulence;
4- The position and dimensions of the air return grille; and
5- Conditions of air on both sides of the air curtain.

All of the above parameters are functions of the design and application of the air curtain. In most cases, the prediction of their performance in standard applications relies on curves supplied by the manufacturer. A number of mathematical models have been developed to aid the design and performance prediction of air curtains. Major contributions to the work include those of Hetsroni [2], Hayes [3] and Van [4].

Hetsroni [2] worked with a recirculatory type air curtain and developed an entrainment spill model to calculate the heat transfer through the air curtain. His simulation results were taken to predict the heat transfer with an accuracy of 20% compared to measurements in the laboratory. Hayes [3] investigated heated non-recirculated air curtains. He developed a model to predict the total heat transfer across the air curtain and used it to investigate the effect of various design parameters such as jet angles, initial velocities and jet temperatures on heat transfer.

Similar to Hetsroni's model, Hayes' model assumed Low initial turbulence intensities, less than 1%, and uniform initial velocity profiles. Following to Hayes' work, Van [4] developed a model to investigate the influence of the initial turbulence intensity of heat and mass transfer through an air curtain. The experimental and modeling results showed that initial turbulence intensity would have little effect on the heat and mass transfer through long air curtains.

The model developed by Van [4] was subsequently applied by Howell and Adams [5] to investigate heat and moisture transfers across air curtains employed on refrigerated display cabinets. Tests carried out on two different air curtain lengths at different room and display cabinet conditions showed differences between computed and measured heat transfers of between 0.7% and 26.5%. Reasons for the errors were not reported but measurement errors would have a significant effect on the overall accuracy of the results.

Cortella et al. [6] worked with a finite element method to analyze the distribution of velocity and temperature in refrigerated display cabinet. They found that when the air velocity at the inner curtain was lower than outer one, multiple air curtains led to a lower air spillage from air curtain to the floor.

Navaz et al. [7] used both experimental and numerical methods to predict the parameters those have significant effects on the amount of warm air in an open refrigerated display case. They found that the turbulence intensity, the mean velocity profile at the discharge air grill and the Reynolds number are main factors those are responsible for the amount of warm air in a display case. The results showed that lowering Reynolds number of the air curtain reduces the entrainment (warm) rate.

Yu et al. [8] established a modified two-fluid turbulence model to simulate the flow and heat transfer characteristics of air curtains in an open vertical display cabinet. The air exiting the back panel, the inner air curtain and the outer air curtain are taken as the first fluid and described with the standard k-ε turbulence model. The air outside the display cabinet is considered as the second fluid and calculated by the laminar model. The results of comparisons between the simulated temperatures and the experimental ones showed that the modified two-fluid model (MTF) could give better agreement with the measurements than k-ε and two original two-fluid models.

Agaro et al. [9] simulated the air flow pattern and the temperature distribution in a frozen food vertical display cabinet. At first the choice of solver parameters has been investigated in a 2D modelisation. 3D simulations have been performed to predict the effects of the cabinet length, the warm air curtain temperature and of longitudinal ambient air movement on the performance of air curtain. The results indicate that, in short cabinets, 3D secondary vortices at the side walls provide the most important mechanism for hot air entrainment. Comparison with experimental resulted showed that a 2D simulation is totally inadequate for such configurations while 3D computations predict refrigeration power within engineering accuracy.

Up to date, most researches on refrigerated display cabinets were focused on computational fluid dynamics (CFD) simulation and experimental studies mainly concentrated on the effects of air supply velocity and initial turbulent intensity on the development of an air jet for one air curtain or two air curtains separately [10-12].

The main objective of the present study is to get the lowest temperature in vertical multi-deck open cabinet using two air curtains at different ambient temperature and relative humidity by reducing the external air infiltration and consequently reduction of energy consumption and comparing the results with a single air curtain

2. Description of flow patterns

The flow patterns of one and two parallel air curtains are shown schematically in Figs. (1) and (2). For one air curtain, flow is divided into three regions, potential core region, transition region and developed region, see Fig. (1). The characteristic of the potential core region is that the centerline velocity is almost constant and equal to the outlet velocity u_o. Also the turbulence intensity is constant. The length of this zone is about 5:8 times the jet thickness b_o [1].

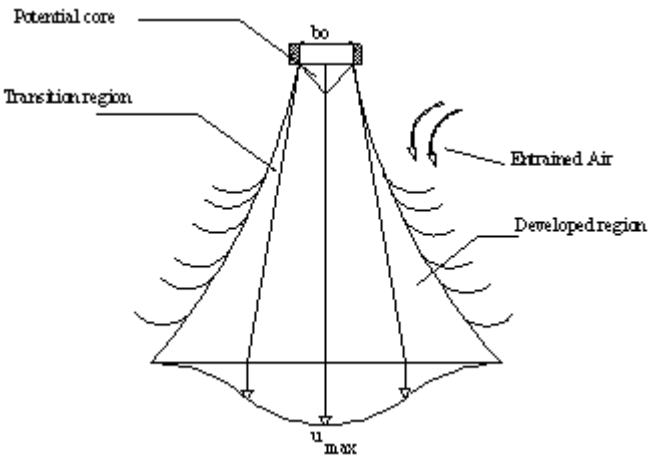

Fig. (1) Flow patterns of one air curtain

As a result of the combined entrainment between the two jets of air curtains, a sub-atmospheric pressure region is formed close to curtain outlet. The sub-atmospheric pressure causes

individual jets, which known as the converging region, see Fig. (2). The two potential cores of the two air curtains combine at merging point where the centerline velocity is zero. This point is called merging point. Downstream from the merging point, in the merging region, the two air jets continue to interact with each other and the centerline velocity increases until it reaches a maximum value at the combined point. Downstream from the combined point, the two air jets combine together to be like a single free jet flow.

Transition region starts with the velocity decay and the amplification of the jet expansion. It generally starts after approximately $5b_o$ from the jet outlet. Developed region velocity decay remains constant. Velocity decay is expressed with non-dimensional quantities. It generally starts after approximately 20 b_o from the jet outlet [1].

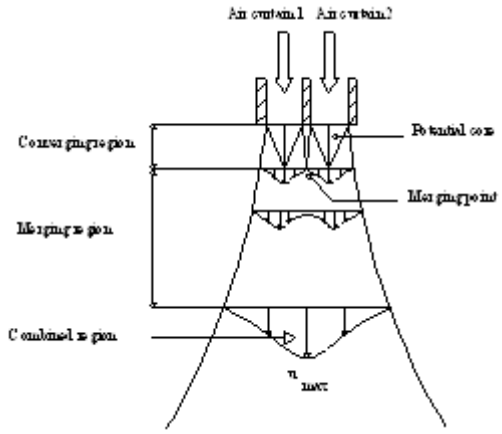

Fig.(2) Flow patterns of the two parallel air curtains

In a vertical open display cabinet which uses two air curtains, for inner air curtain, the air is forced by propeller fans to flow through an evaporator at the bottom of the cabinet. Cooled air is fed into the cabinet through the back panel of the cabinet, and then it is blown through two honeycombs to form two air curtains. The outer air curtain entrains ambient air and spills it to the ground. The inner air curtain is re-cooled by the evaporator while the outer air curtain is bypassed across the evaporator in the air flow tunnel, which makes the temperature of the inner air curtain lower than that of the outer air curtain. The air flow from the perforated back panels can provide cooling for the rear products to avoid cold curtains being prevented by front products. In addition, it can also support the flow of vertical air to perform better insulation performance.

3. Mathematical model formulation

The present numerical study has been based on solving the governing equations those describe airflow inside the refrigerator using one or two air curtains by a CFD program FLUENT 6.2 [13]. This numerical approach solves the partial differential equations governing the transport of mass, three momenta, energy and species in a fully turbulent three dimensional domains under steady state conditions in addition to standard *k*–ε model equations for turbulence

3.1 Governing equations:

In order to choose a CFD model for the refrigerated display cabinet, it is first necessary to decide on a suitable turbulence model, for the particular application. The main criteria which have to be satisfied by the model are:

1. The model must be suitable for low Reynolds number flows;
2. The model must be able to cope with buoyant flows; and
3. The model must be able to cope with separation regions, etc. in complicated geometries.

In order to predict air velocity and temperature in the open refrigerated display cabinets, the momentum, continuity and energy equations have to be solved simultaneously. The different governing partial differential equations are typically expressed in a general form as:

$$\frac{\partial}{\partial x}\rho U\ \Phi+\frac{\partial}{\partial y}\rho V\ \Phi+\frac{\partial}{\partial z}\rho W\ \Phi=\frac{\partial}{\partial x}\left(\Gamma_{\Phi,eff}\frac{\partial\Phi}{\partial x}\right)+\frac{\partial}{\partial y}\left(\Gamma_{\Phi,eff}\frac{\partial\Phi}{\partial y}\right)+\frac{\partial}{\partial z}\left(\Gamma_{\Phi,eff}\frac{\partial\Phi}{\partial z}\right)+S_\Phi \quad (1)$$

Where ρ is the air density and Φ is the dependent variable, S_Φ = Source term of Φ, and U, V, W are the velocity vectors, and $\Gamma_{\Phi,\text{eff}}$ is the effective diffusion coefficient. The effective diffusion coefficients and source terms for the various differential equations [14] are listed in the table 1. Where; μ_t is the turbulent eddy viscosity, μ_e is effective viscosity and ε is the dissipation rate of turbulence kinetic energy and G is the rate of generation of the turbulence kinetic energy (TKE) while ρε is its destruction rate.

Table (1) Terms of partial differential equations (PDE).

	Φ	$\Gamma_{\Phi,eff}$	S_Φ
Continuity	1	0	0
X-momentum	U	μ_{eff}	$-\partial P/\partial x+\rho g+S_U$
Y-momentum	V	μ_{eff}	$-\partial P/\partial y+\rho g(1+\beta\Delta t)+S_V$
Z-momentum	W	μ_{eff}	$-\partial P/\partial z+\rho g+S_W$
H-equation	H	μ_{eff}/σ_H	0

k-equation	k	μ_{eff}/σ_k	$G-\rho\varepsilon$
ε-equation	ε	$\mu_{eff}/\sigma_\varepsilon$	$C_1\varepsilon G/k - C_2\rho\varepsilon^2/k$
$\mu_{eff}=\mu_{lam}+\mu_t$			$\mu_t=\rho C_\mu k^2/\varepsilon$
$G=\mu_t\left[\begin{array}{l}2\left\{(\partial U/\partial x)^2+(\partial V/\partial y)^2+(\partial W/\partial z)^2\right\}+\\(\partial U/\partial y+\partial V/\partial x)^2+(\partial V/\partial z+\partial W/\partial y)^2+(\partial U/\partial z+\partial W/\partial x)^2\end{array}\right]$			
$S_U=\partial/\partial x\left(\mu_{eff}\,\partial\Phi/\partial x\right)+\partial/\partial y\left(\mu_{eff}\,\partial\Phi/\partial x\right)+\partial/\partial z\left(\mu_{eff}\,\partial\Phi/\partial x\right)$			
$S_V=\partial/\partial x\left(\mu_{eff}\,\partial\Phi/\partial y\right)+\partial/\partial y\left(\mu_{eff}\,\partial\Phi/\partial y\right)+\partial/\partial z\left(\mu_{eff}\,\partial\Phi/\partial y\right)$			
$S_W=\partial/\partial x\left(\mu_{eff}\,\partial\Phi/\partial z\right)+\partial/\partial y\left(\mu_{eff}\,\partial\Phi/\partial z\right)+\partial/\partial z\left(\mu_{eff}\,\partial\Phi/\partial z\right)$			
Turbulence model constants C_1=1.44, C_2=1.92, C_μ=0.09			
σ_H=0.9, σ_k=0.9, σ_ε=1.225			

When CFD model is applied to the vertical display cabinet, the following assumptions are made:

1. A steady three-dimensional model is employed regardless of the display cabinet length.
2. The standard k-ε two equations model (k-ε) is selected to simulate the turbulent fluid.
3. Radiation heat transfer is not taken into consideration.
4. The Boussinesq hypothesis is selected due to the density varying with aerostatic pressure.

3.2 Boussinesq approximation

The basis of this approximation is that there are flows in which the temperature varies little, and therefore the density varies little. Thus the variation in density is neglected everywhere except in the buoyancy term. Natural convection was considered by using the Boussinesq approximation in which density was treated as a constant value in all solved equations except for the buoyancy term in the momentum equations which was treated as: $(\rho_o-\rho)g=\rho_o\beta(T-T_o)$, where ρ_o and T_o are the reference density and temperature respectively and $\beta=1/T_o$ is the thermal expansion coefficient

3.3 Buoyancy

The purpose of the air curtain is to provide a momentum force to resist the buoyant force caused by the difference in density and temperature between the air inside and outside of the cabinet. The buoyant force, therefore requires modeling to predict the system. The air in this model is treated as an ideal gas where its density is linked to the temperature by the ideal gas law:

$$P=\rho RT \qquad (2)$$

A numerically simpler approach is to use the Boussinesq approximation:

$$(\rho_o-\rho)g=\rho_o\beta(T-T_o) \qquad (3)$$

This model uses a constant density fluid. The Boussinesq approximation is suitable only if density variations are small.

3.4 Boundary conditions

The velocities and the temperatures of the air curtains are given in Table 2. The inlet turbulent kinetic energy k_{inlet} and the energy dissipation rate ε_{inlet} of the air curtain are derived from the following relationship:

$$k_{inlet}=0.01\,u_o^2 \qquad (4)$$

$$\varepsilon_{inlet}=0.01\,k_{inlet}^{3/2}/b_o \qquad (5)$$

Where u_o is the inlet velocity of the air curtain and b_o is the width of the air curtain (either the inner air curtain or the outer air curtain). Non-slip boundary condition (zero velocity) is selected at the solid surfaces.

The following table (2) gives the values under a typical display case operation condition.

Table (2) Principal parameters of the display case

Parameters	Values
Display case width W (m)	0.61
Display case height H (m)	0.45
Inner air curtain width $b_{o,in}$ (m)	0.03
Outer air curtain width $b_{o,out}$ (m)	0.03
Ambient temperature T_a (^oC)	20
Ambient relative humidity (%)	45
Outer air curtain velocity $u_{o,out}$ (m/s)	0.69
Inner air curtain velocity $u_{o,in}$ (m/s)	0.69
Outer air curtain temperature T_{out} (^oC)	4.4
Inner air curtain temperature T_{in} (^oC)	11

The computer program, FLUENT 6.2 was used to solve the time-independent (steady state) conservation equations together with the standard k-ε model, and the corresponding boundary conditions. The numerical solution grid divided the space of the cold room into discretized computational cells of the order of 500,000 tetrahedral cells. Solution convergence criteria, was applied at each iteration and ensured the summations of normalized residuals were less than10^{-4} for flow, 10^{-4} for k and ε, and 10^{-6} for energy.

4. Experimental Setup

The apparatus on which the experimental work has been conducted was built in heat engine laboratory, Faculty of Engineering at Shebine El-Kom, Egypt. It was a single deck, vertical viewer

refrigerator that shown in Fig. (3). The unit consists of a vertical cabin supplied with a refrigeration unit. The cabinet was made of steel - polyurethane panel. The outer and inner sides of the cabin were made of 1 mm wall thickness steel sheet. The polyurethane insulation used was of 50 mm thickness and it has thermal conductivity of 0.025 W/m.K.

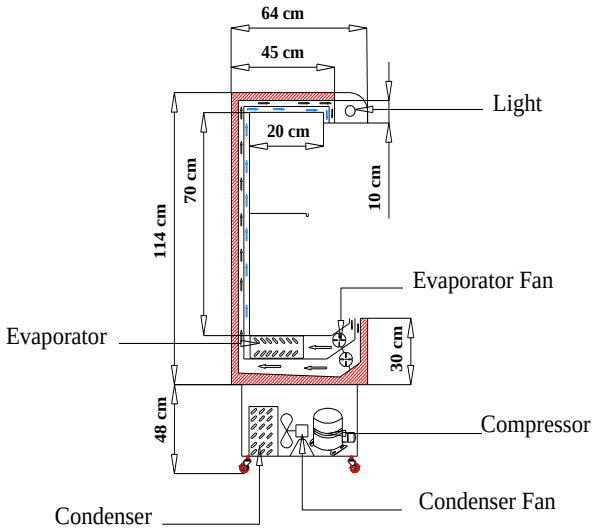

Fig. (3) Test section

The refrigeration unit consists of an evaporator, a compressor 550 W, a condenser and an expansion device. The outer dimension of the display cabinet is 1.2m, 0.63m and 0.72m long. Two fans were installed to provide the required air in the cabinet, one of them was fixed before the evaporator in first duct while the last one was fixed inside the second duct. The air curtain width were 13 and 5 cm for both one and two air curtains. The back panel width and top ceiling gap were 50mm.

The test section was installed inside an isolated room of 2.5×1.5×2 m. The room was made of steel-Polyurethane panel with 5 cm insulation. It was supplied with a split air conditioning unit of 1.125 kW electric power consumption, a humidifier, electric heater and relative humidity and temperature controls and to maintain the inside room at the required various test conditions as defined by the ISO test standard.

In order to measure the temperature distribution inside and outside the display cabinet, thermocouples of K-type were distributed inside it as shown in Fig. (4). The measuring range of that type is -50^{o}C to 200^{o}C. The thermocouples were chicked for damage before installation. The output signals of the thermocouples were transferred to a digital temperature indicator set. The relative humidity was measured by digital hegrostate at the same lacations of temperature measurement. A cup anemometer was also used to measure the air flow velocity at the same locations.

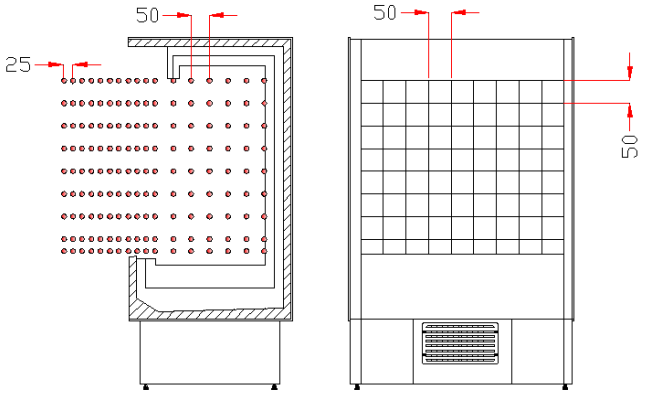

Fig. (4) Positions of measuring the velocity, temperature and relative humidity of air.

5. Results and Discussion

Figure (5) indicates a comparison of predicted velocity distribution u/u_o between the experimental work and four numerical models, they are; k-ε model and k-Ω model, laminar model and Reynolds stress model (RSM). Laminar model is less accurate because the flow may be more turbulent in this region. The other three of the turbulence models predicted this velocity gradient much better. The theory of turbulent jets suggests that an initial region of the jet exists before the turbulence region (laminar region due to honeycomb). As the air curtain develops downstream of the outlet, the centerline velocity decays and the pattern of the air flow spreads. It then follows that small eddies in the flow direction into larger ones increasing the length scale and resulting in a higher Reynolds number. It seems, therefore, that the flow is becoming more turbulent. Both k-ε and k-Ω models provided the best prediction of the velocity profile at mid of air curtains. k-ε model is chosen for this present work as it is more accurate and it was used in most previous researches.

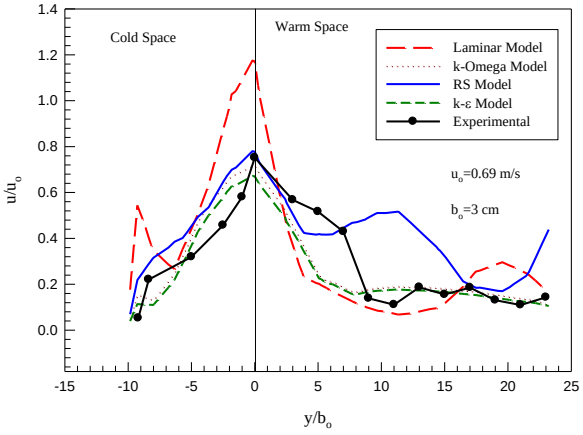

Fig. (5) Comparison of velocity profiles at x/b_o =12, two air curtains.

5.1 Velocity distribution for two air curtain

Figure (6) gives the contours of velocity in both refrigerator and test room. For vertical multi-deck cabinet considered here, the cold air is blown through two linear diffusers placed in front of the canopy, to form the two air curtains. Each linear diffuser is supplied by a separate fan, where a honeycomb panel ensures a uniform air distribution and an accurate control of the jet velocities.

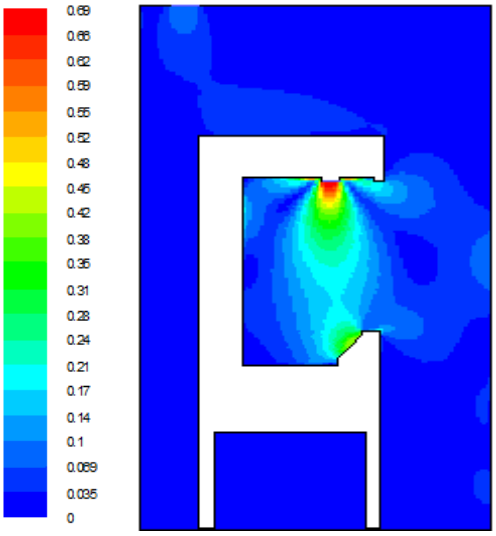

Fig. (6) Contours of velocity of air through air jets

5.2 Comparison between the air velocity distributions through one and two air curtains

Figures (7), (8) and (9) represent the comparison of velocity profiles at x/b_o=6, 12 and 20 respectively, for the case of one air curtain and two air curtains. From the comparison of the results, it is found that at x/b_o=6 the velocity profile at the case of two air curtains are greater than the velocity profile for one air curtain. This is because of the air entrainment at outer air curtain which spills out of the refrigerator. At the same time the inner air curtain spills inside the refrigerator, which lead to keep the inside temperature cool and constant. Consequently, the velocity is decreased slightly. At one air curtain the air entrainment occurred where part of the air curtain spills out the refrigerator and the other part combined with some of outside air is induced inside the refrigerator, which means increasing the temperature inside the refrigerator and the velocity decreases due to air entrainment.

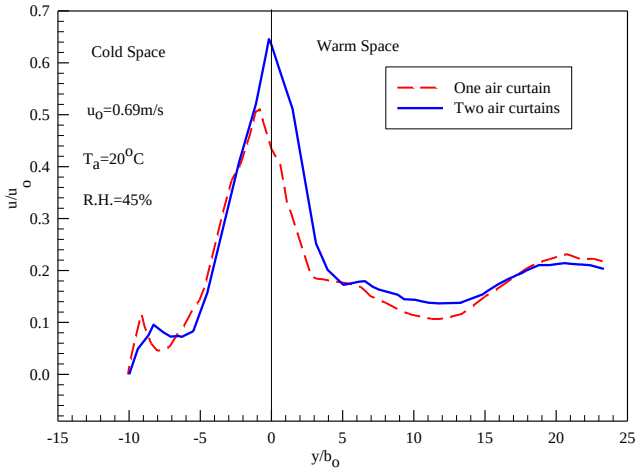

Fig. (7) Comparison of velocities distributions of one and two air curtains at x/b_o=6.

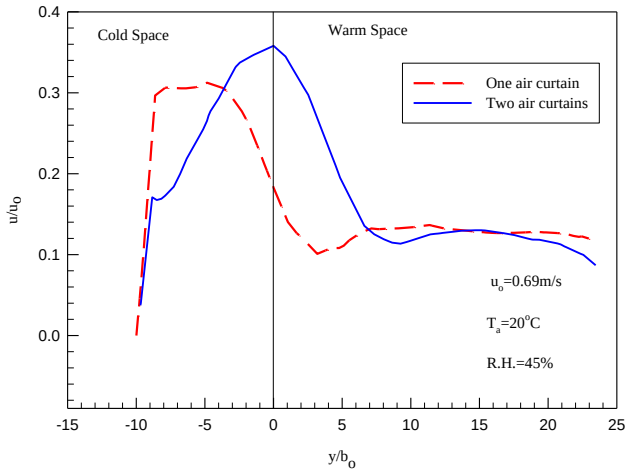

Fig. (8) Comparison of velocities distributions of one and two air curtains at x/b_o=12.

From Fig. (9) it can be seen that at y/b_o equal to about 6, where outside air is combined with air curtain there is circulation due to the fan suction.

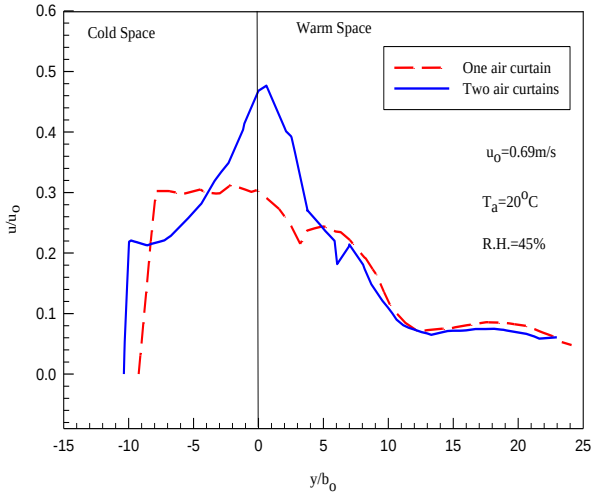

Fig. (9) Comparison of velocities distributions of one and two air curtains at x/b_o=22.

5.3 Comparison of the temperature Distribution in cases of one and two air curtains

Figures (10), (11) and (12) illustrate the temperature distribution for one and two air curtains. It can be seen that in the display cabinet of using the two air curtains the temperatures inside the fridge is cooler than that inside the fridge using one air curtain as mentioned previously. Also, it can be seen that as x/b_o is increasing the value of T/T_o decreases in the fridge with two air curtains. At $y/b_o=6$, T/T_o in both one air curtain and two air curtains is the same due to the velocities of air curtains at maximum value and uniform so that the air entrainment does not start. On the other hand, it can be seen also that as y/b_o increases, T/T_o increases due to same previous reason.

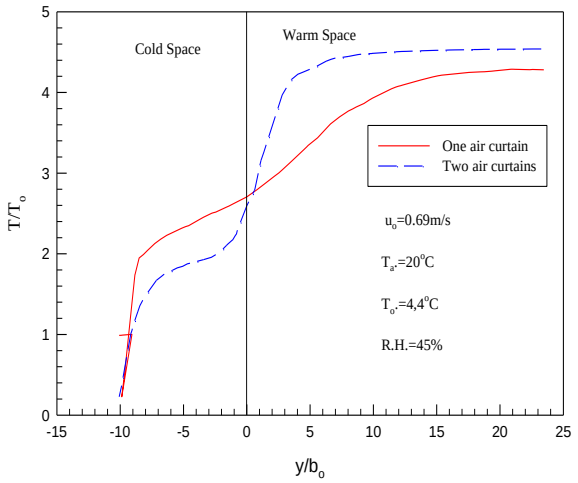

Fig. (10) Comparison of air temperatures distributions of one and two air curtains at $x/b_o=3$

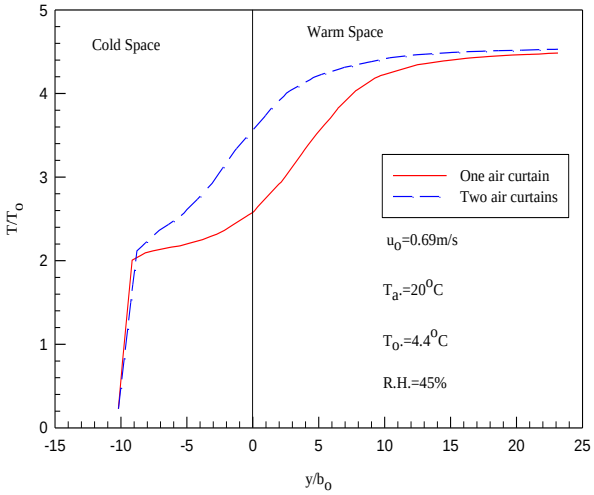

Fig. (11) Comparison of air temperatures distributions of one and two air curtains at $x/b_o=12$

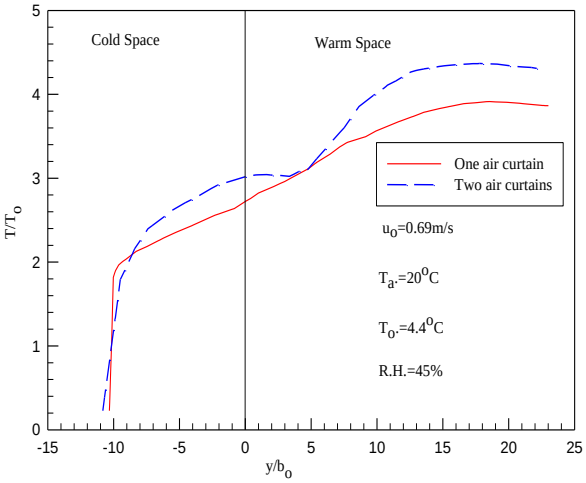

Fig. (12) Comparison of air temperatures distributions of one and two air curtains at $x/b_o=20$

5.4 Comparison between humidity ratio distributions through one and two air curtains

The simulations were carried out with air curtain temperature of 4.4°C which discharge from outlet and ambient temperature 20°C and relative humidity 45% at different x/b_o and y/b_o. The following Figures illustrated the influence of ambient conditions on humidity ratio through one and two air curtains.

As shown in the following Figs (13), (14) and (15), it can be seen that the effect of ambient conditions on humidity ratio inside the fridge. It was shown that the humidity ratio inside the fridge is lower in the case of using two air curtains is lower than that in the fridge uses one air curtain. Also, it can be seen that, as y/b_o increases the humidity ratio ω/ω_o is increased for both one and two air curtains.

As shown from Fig. (13) it can be seen that ω/ω_o in the case of one air curtain near the back of the fridge is lower than ω/ω_o in the case of two air curtain, this is because the temperature through duct at x/bo=3 in the case of two air curtains is higher than one air curtain. And as x/bo increases the temperature in the duct will decrease (at y/bo=-10).

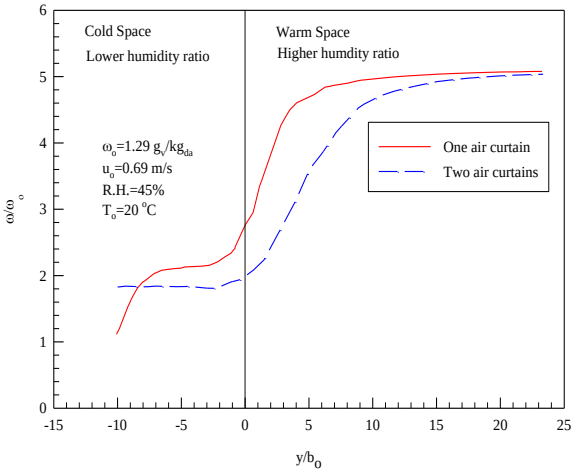

Fig. (13) Comparison of humidity ratio distributions of one and two air curtains at x/b_o=6

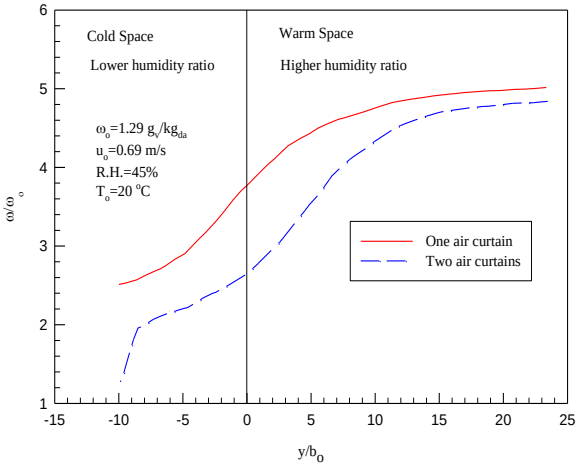

Fig. (14) Comparison of humidity ratio distributions of one and two air curtains at x/b_o=12

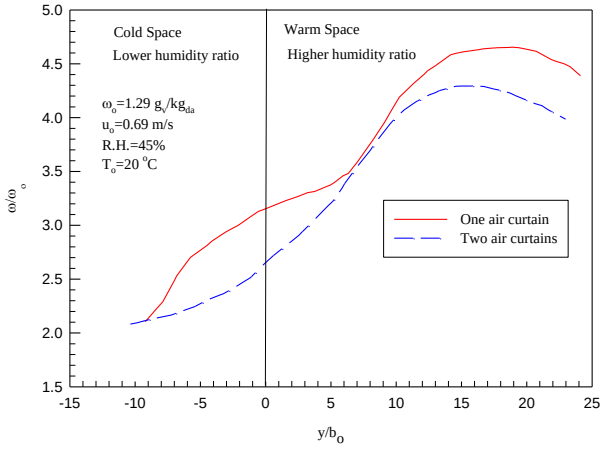

Fig. (15) Comparison of humidity ratio distributions of one and two air curtains at x/b_o=22

6. Heat transfer calculation model

The entrainment-spill model is similar to that used by Hetsroni [2] for the recirculatory type air curtain. Hetsroni proposed that, the main heat transfer mechanism is due to heated air from the room being entrained into the jet, and then it is cooled, and spilled back into the room again at a lower temperature. The heat transfer rate can be calculated from the velocity and temperature distributions at a jet cross-section just before the impingement point as shown in Fig. (16). The heat transfer model depends on the effect of temperature and humidity ratio differences between the two sides of the air curtain. As shown in Figs. (1) and (2), the two air curtains can be dealed as one air curtain.

The flow pattern of the air curtain can be divided into two parts. The first part is the secondary air entrained from each side (cold space and warm space). This part causes the divergence of the air curtain jet and it spills back at the floor level (with different conditions) to the side from which it comes. Therefore, it causes heat transfer to this side, see Fig. (16). The second part is the primary air that is used in the air curtain outlet which may come from one side of the curtain (cold space and warm space). This air comes with certain conditions (T and HR) and used in curtain. These conditions will be changed when it spills back at the floor level to the side from which it comes. This change will cause certain heat load on this side.

The heat transfer rate can be calculated from the velocity and temperature distributions at a jet cross-section just before the impingement point shown in Fig. (16).

The sensible heat transfer rate for air curtain side, depending on the temperature of this side T_{side} (cold space or warm space), and can be given by [2]:

$$\dot{Q}_s = \dot{Q}_{s(Sec)} + \lambda \dot{Q}_{s(\mathrm{Prim})} \qquad (6)$$

Where λ is a factor equal to 1 in case of heat transfer calculation for the side from which the primary air comes and it is equal to (0) if the heat transfer calculation is for the other side.

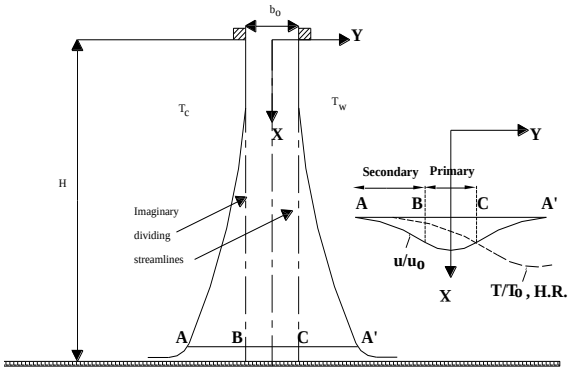

Fig. (16) Description of heat transfer model

$$\dot{Q}_s = \dot{m}_{a(Sec)} C_p (T_{side} - T(Y)_{Sec}) + \lambda \dot{m}_{a(Prim)} C_p (T_o - T(Y)_{Prim}) \quad (7)$$

Where T_o is the outlet temperature of the air curtain.

$$\dot{Q}_s = W \int_{y_A}^{y_b} \rho C_p u(y)(T_{side} - T(y)_{sec}) dy + \lambda W \int_{y_A}^{y_b} \rho C_p u(y)(T_o - T(y)_{prim}) dy$$

(Just before the impingement point at X = H)

Equation (8) represents the difference betwee the dry air enthalpy of the entrained air into the j from air certain side and enthalpy of dry air on th side. Also the difference between the enthalpy primary air used in the curtain, that spilled back in this side again just before the impingement poir with the enthalpy of dry air on this side. Tw assumptions are involved in this equation:

1. The length of the entrainment zone, measured along the axis of the jet, is H, regardless of the amount of deflection of the jet. This means that the location of section AA' of the jet shown in Fig. (16) will always lie slightly above the floor because of the curvature of the jet.
2. The velocity and temperature distributions for the air spilling back into the space are the same as those between points A and A', Fig. (16).

From convection heat transfer, a heat transfer coefficient, h, is defined by

$$\dot{Q}_s = h(H.W)(T_w - T_c) \quad (9)$$

If the specific heat is assumed constant and an average value is used for the air density, applying the mass conservation (at outlet of air curtain at level B-C) and stream function definition at $Y_C = Y_B$: it will obtain $\psi_C = 0.5$, $\psi_B = -0.5$.

$$\frac{Nu}{\mathrm{Re.Pr}} = \int_{\mp\psi_A}^{\mp 0.5} (\theta)\, d\psi + \lambda \int_{-0.5}^{0.5} (\theta)\, d\psi \quad (10)$$

The negative sign is used for the secondary part for calculating the sensible heat transfer for the left side, and the positive sign is used for right side in Fig. (16).

By solving Equations (9) and (10) using the compound Simpson method of integration. The values of (Nu/RePr) for different values of opening height H or (H/b_o) can be calculated. From Fig. (17) it is shown that the ratio Nu/Re.Pr is greater in primary air, and increases as H/b_o increases due to entrained air from warm space section C-A' Fig.(16). Although the ratio Nu/Re Pr in secondary air increases with H/b_o, but it is lower than in primary air. This is because of the amount of entrained air from cold space section A-B Fig. (16).

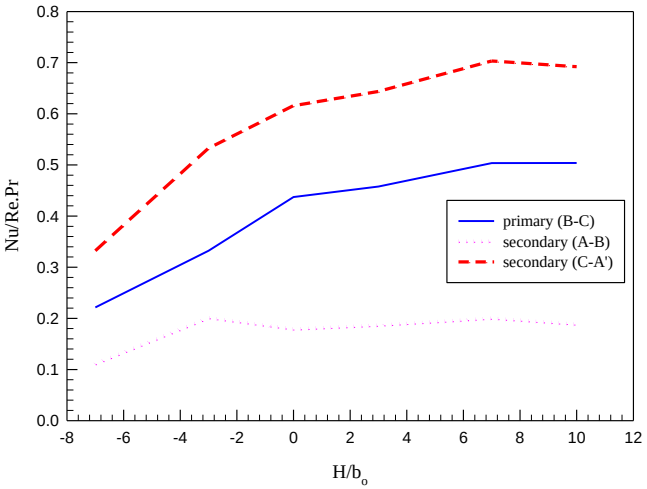

Fig. (17) Variation of (Nu/Re.Pr) with H/b_o

The results obtained could be fitted and the following equation is obtained:

$$\frac{Nu}{Re.Pr} = 0.6069 + 0.0256 \frac{H}{b_o} - 0.00175 \left(\frac{H}{b_o}\right)^2 \quad (11)$$

From Nu/Re Pr, the value of heat convection coefficient could be obtain as following:

$$h = \frac{\rho_{av}\, u_o\, b_o\, C_p}{H} \frac{Nu}{\mathrm{Re.Pr}} \quad (12)$$

The values of ρ_{av} and C_p almost constant and equal to 1.15 kg/m^3 and 1.005 KJ/kg.K respectively. The obtained value could be substituted in Eq. (13);

$$\dot{Q}_s = hA\Delta T \tag{13}$$

Then:

$$\dot{Q}_s = \pm\rho_{av} C_p u_o b_o W (T_w - T_c) \times [0.6069 + 0.0256\frac{H}{b_o} - 0.00175(\frac{H}{b_o})^2] \tag{14}$$

The positive sign is used for the sensible heat added to the cold side and the negative sign is used for the sensible heat loss from the warm side.

6.2 Latent Heat Transfer Calculations

The latent heat transfer rate can be calculated from the velocity and humidity ratio distributions at a jet cross-section just before the impingement point see Fig. (16). Where the latent heat transfer rate is given by:

$$\dot{Q}_L = \dot{Q}_{L(Sec)} + \lambda \dot{Q}_{L(\mathrm{Prim})} \tag{15}$$

The rate of mass convection can be expressed as:

$$\dot{m}_{Conv} = h_{mass}\rho A(\omega_{higher} - \omega_{lower}) \tag{16}$$

$$\dot{Q}_L = \dot{m}_{conv}\, i \tag{17}$$

and enthalpy of moist air can be expressed as [15]:

i=2502+1.84T

$$\dot{Q}_s = W\int_{y_A}^{y_b} \rho i u(\omega_{side} - \omega(y)_{\mathrm{sec}})dy + \lambda W\int_{y_A}^{y_b} \rho i u(\omega_o - \omega(y)_{prim})dy \tag{18}$$

(Just before the impingement point) at X = H,

Appling the mass conservation (at outlet of air curtain and level (B-C) and stream function definition at Y_C=Y_B: ω_{higher}=ω_{lower} it will obtain ψ_C=0.5, ψ_B=-0.5.

$$\dot{Q}_L = W u_o b_o i\, \rho_{av} [\int_{\mp\psi_A}^{\mp 0.5} (\omega_{side} - \omega(y)_{sec})\, d\psi + \lambda \int_{-0.5}^{0.5} (\omega_{side} - \omega(y)_{prim})\, d\psi] \tag{19}$$

$$\dot{Q}_L = \rho_{av}\ h_{mass}\ H\, W\left(\omega_{higher} - \omega_{lower}\right) i \tag{20}$$

From Fig. (18) the results obtained could be fitted in order to obtain the following equation

$$\frac{Sh}{\mathrm{Re.Sc}} = 0.1726 + 0.0594\ \frac{H}{b_o} - 0.001714\ \left(\frac{H}{b_o}\right)^2 \tag{21}$$

Substituting Sh , Re and Sc numbers in Eq. (20) gives:

$$h_{mass} H = u_o\ b_o\ \frac{Sh}{\mathrm{Re}Sc} \tag{22}$$

Then:

$$\dot{Q}_L = \pm u_o b_o \rho_{av} h_g (\omega_{higher} - \omega_{lower}) \times [0.1726 + 0.0594\frac{H}{b_o} - 0.001714(\frac{H}{b_o})^2] \tag{23}$$

The positive sign is used for the latent heat added to relatively low humidity ratio and the negative sign is used for the latent heat loss from relatively high humidity ratio.

$h_{heat} \cong \rho\, C_p h_{mass}$ (Air-water vapor mixtures)

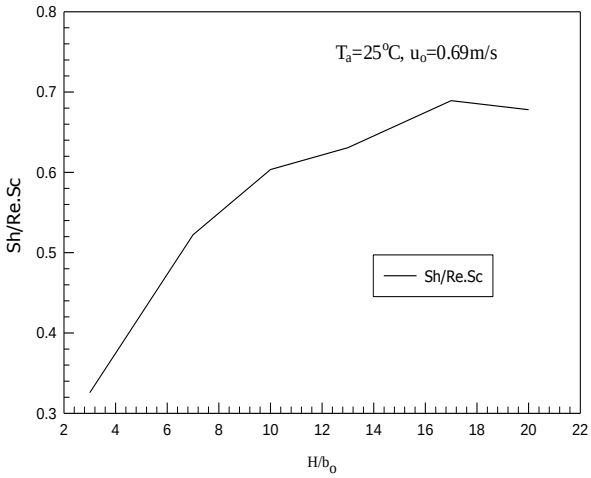

Fig. (18) Variation of Sh/Re Sc with H/b_o at T_a=25^{o}C, u_o=0.69m/s

6.3 Relation between heat transfer Stanton number and mass transfer Stanton number

As mentioned previously the mass transfer Stanton number is close to the heat transfer Stanton number at different values and as shown in Fig. (19).

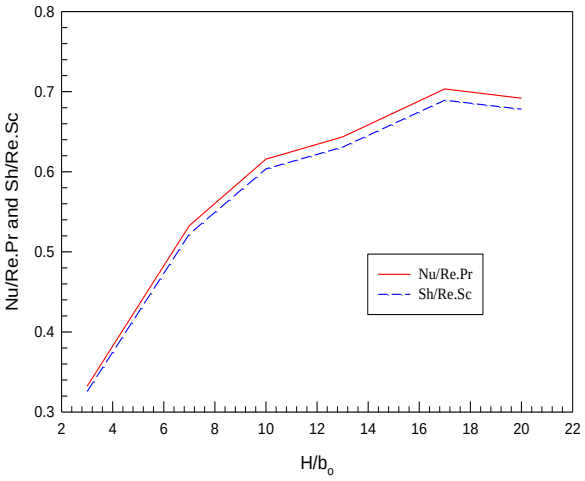

Fig. (19) Relation between Nu/Re .Pr and Sh/Re .Sc at different values H/b_o

Figure (20) shows the comparison between sensible heat transfer through one air curtain and two air curtains at different ambient temperatures. It is shown that the fridge which equipped with two air curtains had low sensible and latent heat transfer comparing with the fridge equipped with one air curtain. Figure (21) describes the heat and mass transfer through the two air curtains at different values H/b_o. Therefore, the increase of ambient temperatures and relative humidities lead to increase sensible and latent heat.

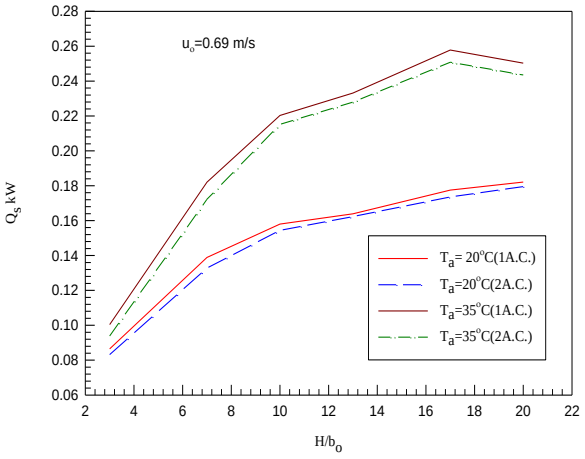

Fig. (20) Comparison of Q_s of one and two air curtains at different values of H/b_o

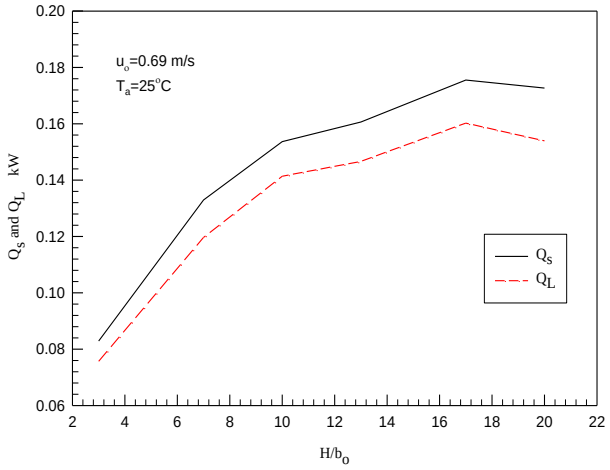

Fig. (21) Relation between Q_s and Q_L at different values H/b_o

The sensible heat transfer obtained from this work is compared with that obtained by G. Verthaeghe [17] and C. Rey [16] and plotted in Figs (22) and (23). The comparison indicates that, the data between the present work and other research were close to each other.

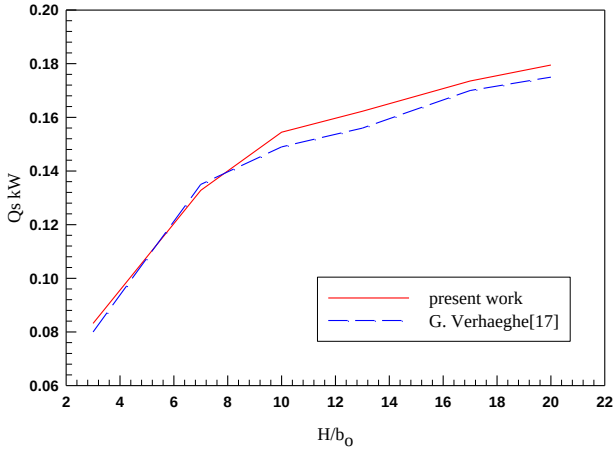

Fig. (22) Variation of Q_s through one air curtain

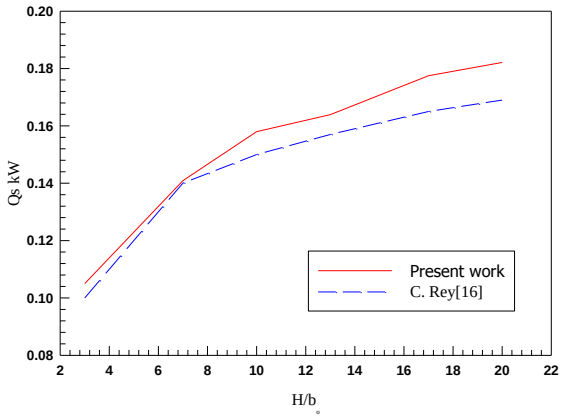

Fig. (23) Variation of Q_s through two air curtains

7. Conclusions

The numerical study on vertical air curtains for multi-deck viewer refrigerated display shows some of the most important factors and parameters that clearly affect the design of the air curtains, its performance and its function to seal a refrigerated space from ambient conditions. From the analysis of the results presented in this study, the following conclusions may be drawn:

1- The air curtain design parameters such as curtain outlet thickness (b_o) and outlet velocity u_o have a great effect on the heat and mass transfer rate through the air curtain.
2- The decrease of outlet thickness and velocity of the air curtain increases led to increase of the heat and mass transfer rate.
3- To overcome the increase of the difference between the refrigerated space and ambient conditions, small air curtain thickness and higher outlet velocity are used in the two cases of one air curtain and two air curtains.
4- Using the two air curtains leads to decrease the temperature and humidity ratio inside the fridge and tends also to decrease the power consumption than the case of one air curtain.
5- Using two air curtains into a display cabinet, enhances the performance of the unit is increased when the velocity of outlet air curtain is higher than the velocity of the inlet air curtain.

Nomenclature:

Symbol	Quantity
A	Area, m^2
AC	Air curtain
Cp	Specific heat at constant pressure, kJ/kg.K
D	Diffusion coefficient, m^2/s
H	Display cabinet height, m
h	Convection heat transfer coefficient, $W/m^2.K$
h_{mass}	Mass transfer coefficient, m/s
I	Enthalpy of moisture, kJ/kg
k	Kinetic energy
$\dot{m}_{conv}$	Rate of mass convection, kg/s
Nu	Nusselt number
P	Absolute pressure, N/m^2
Pr	Prandtl number
$\dot{Q}$	Heat transfer, kW
R	Individual gas constant, J/kg.^oK
Re	Reynolds number
RH	Relative humidity
Sc	Schmidt Number
Sh	Sherwood Number
St_{mass}	Mass transfer Stanton number, Sh/Re.Sc
S	Source of term Φ
T	Temperature, k
U	Velocity vector in X direction
u	Velocity, m/s
V	Velocity vector in Y direction
W	Width of air curtain, m

Greek Letters

β	1/T
Γ	Diffusion coefficient
ε	Energy dissipation rate
θ	Dimensionless temperature = $(T-T_c)/(T_w-T_c)$
λ	Switch factor, 1 or 0
μ	Turbulent viscosity, pa s
ρ	Air density, kg/m^3
ψ	Stream function
ω	Humidity ratio, kg_v/kg_a
Φ	Dependent variable

Subscripts

a	Dry air
av	Average
da	Dry air
eff	Effective
c	Cold
L	Latent heat transfer , kW
o	Curtain outlet
Prim	Primary
s	Sensible heat transfer, kW
Sec	Secondary
t	Turbulent
v	Vapour
w	Warm, water vapor

References:

[1] G. Krajewski, "Efficiency of air curtains used for separating smoke free zones in case of fire" 13th conference of internal building performance simulation association chambery, france, august 26-28, proceeding of bs 2013.
[2] G. Hetsroni, "Heat transfer through an air curtain" Ph. D. Thesis, Michigan State University, East Lansing, 1963.
[3] F. C. Hayes, "Heat transfer characteristics of the air curtain: a plane jet subjected to transverse pressure and temperature gradient" Ph. D. Thesis, University of Illinois, Urbana, IL, 1968.
[4] N. Q. Van, "Influence of initial turbulence intensity on heat transfer through a recirculated air curtain" Ph.D. Thesis, University of Missouri-Rolla, Rolla, MO, 1975.
[5] R. H. Howell, P. Adams, "Effects of indoor space conditions on refrigerated display case performance" Final report for ASHRAE. Project No. 596RP, 1991.
[6] G. Cortella, M. Manzan, and G. Comini, "CFD simulation of refrigerated display cabinets" International journal of refrigeration, vol. 24, pp 250-261, 2001.
[7] HK. Navaz, BS. Henderson, R. Faramarzi, A. Pourmovahed and F. Taugwalder, "Jet entrainment rate in air curtain of open refrigerated display cases" International Journal of Refrigeration, vol. 28, pp 267–275, 2005.
[8] KZ. Yu, GL. Ding and TJ Chen, "Modified two-fluid model for air curtains in open vertical

display cabinets" International journal of refrigeration, vol. 31, pp 472–482, 2008

[9] PD Agaro, G. Cortella and G. Croce, "Two-and three-dimensional CFD applied to vertical display cabinets simulation". International Journal of Refrigeration. Vol. 29, pp 178–190, 2006.

[10] Y. T. GE, S. A. Tassou: "Simulation of the performance of single jet air curtains for vertical refrigerated display cabinets" Applied Thermal Engineering vol. 21, pp 201-219, 2001.

[11] P. E. Ramin Faramarzi: "Efficient Display Case Refrigeration" J. Refrigeration, 1999.

[12] A. Yeo, J. A. Reizes, E. Leonardi, and G. Vahl Davis, "Numerical simulation of refrigerated display cabinet", ASHRAE Transactions 2000.

[13] FLUENT user's guide, Version 6. FLUENT, Fluent, Inc; 2003.

[14] D. B. Spalding, and S. V. Patankar, "A Calculation Procedure for Heat, Mass and Momentum Transfer in Three Dimensional Parabolic Flows" Int. J. Heat & Mass Transfer, 15, pp. 1787, 1974.

[15] Wayne C. Turner and Steve Doty "Energy Management Handbook" 6th edition, Published by the Fairmont Press, Inc., 2006.

[16] M. Pavageau, K. Loubière, A. Koched, F. Aloui, J.C. Elicer-Cortés and C. Rey, "Plane turbulent impinging jets", Turbulence, Heat and Mass Transfer 6, 2009 Begell House, Inc.

[17] G. Verhaeghe, "Study of air curtains used to restrict infiltration into refrigerated rooms". 7th International conference on Heat Transfer, Fluid Mechanics and Thermodynamics, 2010.